Technical paper, submitted to “stahl und eisen” magazine on 8 May 2017

Chromium stability in steel slags

Chromstabilität in Stahlschlacken

by

Dr. mont. Elizaveta Cheremisina, Postdoc at K1-Met GmbH Leoben, Austria, and

Professor Johannes Schenk, Chair of Ferrous Metallurgy, Head of the department of Eisen und Stahlmetallurgie at Montanuniversität Leoben, Austria.

Contacts:

elizaveta.cheremisina@k1-met.com, johannes.schenk@unileoben.ac.at

Abstract

Chromium is an essential element in steelmaking industry. Steel slag inevitably contains some chromium and there is a risk of Cr emission from slag to the environment, however, in which form the emission of the element occurs and whether it is a hexavalent Cr is a concern. To investigate the conditions of hexavalent chromium formation in steel slags and its migration to the atmosphere, an estimation of Cr oxide’s stabilities has been carried out in this paper. Factsage 7.1 has been applied to analyze the thermodynamic properties of Cr oxides with respect to the Cr^{6+} formation. An Ellingham diagram and standard Gibbs free energy change has been proposed. Stability diagrams for BOF, EAF and LF slag systems with various compositions have been derived. Slag basicity was indicated as an influencing factor for Cr containing phase formation. Based on thermodynamic calculations Cr^{3+} phases were determined to be dominant for the given slags and no hexavalent Cr phases were indicated in the real multicomponent slag systems.

German abstract

Chrom ist ein wesentliches Element in der Stahlerzeugung. Stahlwerksschlacken können daher gewisse Anteile an Chrom enthalten und somit ist ein gewisses Risiko der Freisetzung von Chrom in die Umwelt nicht auszuschließen. Von Bedeutung ist daher die Frage, in welcher Form Chrom in Stahlwerksschlacken vorliegt und ob es sich dabei um das gesundheitlich bedenkliche sechswertige Chrom handelt. Gegenstand der vorliegenden Arbeit ist es, die Oxidationsstufen des Chroms in Stahlwerksschlacken und speziell die Bedingungen für die Bildung von sechswertigem Chrom näher zu betrachten. Mittels Factsage 7.1 wurden die thermodynamischen Eigenschaften der verschiedenen Chromoxide in Hinblick auf die Bildung von sechswertigem Chrom analysiert. Ein Ellingham-Diagramm und Änderungen der freien Enthalpie wurden hergeleitet sowie Phasendiagramme für LD-, Elektroofen- und sekundärmetallurgische Schlacken abgeleitet. Die Schlackenbasizität wurde als wesentlicher Faktor für die Bildung Chrom-haltiger Phasen identifiziert. Basierend auf den thermodynamischen Berechnungen wurden Phasen mit dreiwertigem Chrom als die dominierend Chromphasen in den betrachteten Systemen erkannt, wohingegen Phasen mit sechswertigem Chrom sich als nicht stabil erwiesen.

Introduction

Steel slag is a by-product from the crude steel production in basic oxygen converter (BOF converter) and electric arc furnace (EAF) as well as from the secondary metallurgy steel treatment (e.g. ladle furnace). The reuse of slag has been widely applied in many countries. Slags due to their properties can serve a role of a construction aggregate for roads building, soil stabilization, fertilizer or cement production. Although, specifically converter and EAF slags are a perspective building aggregate, its behavior and influence on the environment and human health is a concern [1].

A large number of phases present in the slag including water resistant phases like wuestite or spinel and water soluble phases like merwinite, periclase, dicalcium silicate and lime. Also, metallurgical slag contains potentially harmful elements like chromium. In the case when chromium is not adequately stabilized, it can convert to the hexavalent state by means of oxidation, and leach out, especially in oxygen rich environments. Hexavalent chromium is a well-known carcinogen [1; 2].

Numerous studies [2…4] have been carried out on the topic of chromium immobilization in spinel phase. It was reported that chromium leaching is low when element is bound to the stable spinel phases like $MgCr_2O_4$ or $FeCr_2O_4$.

Kühn et al. [4] has suggested the so called 'factor sp' for EAF slag from stainless steelmaking to describe the factor of spinel forming agents.

$$\text{Factor sp} = 0.2 \cdot MgO + 1.0 \cdot Al_2O_3 + n \cdot FeOx - 0.5 \cdot Cr_2O_3 \text{ [wt.\%]} \quad (1)$$

The following empirical correlation takes into account the spinel factor and chromium leaching levels, where 'n' is a number between 1 and 4, depending on the oxidation state of the slag. An intensive chromium leaching corresponds to the factor sp less than 5 and comparably low leaching when factor sp is greater than 5.

Mudersbach et. al. [5] proposed the addition of Al_2O_3 to the EAF slag from stainless steelmaking to enhance the spinel phase formation.

Another "factor cs" was developed Schüler et al. [6] It allows prognosing the chrome leaching of an EAF slag from carbon steelmaking. If "Factor cs" is greater than 50 % the vast bulk of chromium is bound in solvable calcium silicates, while a low "factor cs" value shows that chromium is bound in unsolvable spinel.

Sano et al. [7] described the oxidation of chromium Cr^{+3} contained in the spinel to Cr^{+6} in stainless steel slag in the air and noted that the Cr^{+6}/ Cr^{+3} raises with the increasing slag basicity CaO/SiO_2. It was also reported that basicity up to a great extent influences spinel stability, thus the formation of hexavalent chromium is favored with increased basicity.

According to Morita et al. [8] oxygen partial pressure also has a great impact on Cr^{+6} formation. In the experimental study of Mg-chromate solubility in slag at temperatures of 1873K depending on oxygen partial pressure, authors observed CrO and Cr_2O_3 at lower partial pressure and Cr_2O_3 and CrO_3 at higher pO_2. Chromium valences of 2+ and 3+ correspond to the lower oxygen partial pressures while the ratio of Cr^{3+}/Cr^{2+} rises with the increasing slag basicity and oxygen partial pressure [2].

There are several experimental studies [2; 7; 8] with consistent results indicating the behavior of CrO_4^{2-} formation based on $Cr_2O_7^{2-}$ ions followed by CrO_3 emissions.

G. J. Albertsson [2] in the study of abatement of chromium emissions from steelmaking pointed out that slow cooling rate of slag at low oxygen partial pressure support the spinel phase precipitation and reduces the Cr dissolution in the water-soluble phases. Author also reported that slag's basicity greater than 1.4 inhibit the formation of the spinel phase at high oxygen partial pressures and hence, high slag basicity leads to the formation of leachable, detrimental chromium-containing phases.

It was also indicated that at high temperatures and oxygen partial pressured the emission of chromium from the stainless steel slag can occur, due to CrO_3 evaporation from the slag surface.

Thermodynamic calculations. Cr stability regions

This paper focuses on the investigation of conditions which would lead to the formation of hexavalent chromium in steel slags using Factsage software. The aim is to provide reliable data according to the thermodynamic properties of chromium oxides with regard to the emissions of toxic hexavalent chromium to the environment. Factsage 7.1 [9] software has been applied for assessment of stability conditions of chromium phases.

Generally, chromium can exist in the following valence states: 0, +1, +2, +3, +4, and +6 with the corresponding oxides Cr_2O, CrO, Cr_2O_3, CrO_2, and CrO_3 respectively.

According to the stability diagram Cr-O_2 (see Fig. **1**) which was plotted using Fact 53 and FToxid databases Cr_2O_3 and CrO_2 oxides are in the solid form at high temperatures of 700-2600K. There is no data indicating CrO_3 oxide on the diagram plotted by FactSage. Researches [2…4; 7; 8] reported the presence of Cr^{6+} at high oxygen potentials.

For the analysis of thermodynamic data the formation of various chromium oxides has to be considered. Chromium oxides form according to the following reactions:

$$4Cr + O_2 = 2Cr_2O \quad (2)$$

$$2Cr + O_2 = 2CrO \quad (3)$$

$$4/3Cr + O_2 = 2/3Cr_2O_3 \quad (4)$$

$$Cr + O_2 = CrO_2 \quad (5)$$

$$2/3Cr + O_2 = 2/3CrO_3 \quad (6)$$

Hexavalent chromium can also form according to the following reaction:

$$2CrO_2 + O_2 = 2CrO_3 \quad (7)$$

To evaluate the assessment of chromium oxide's stabilities, Ellingham diagram has been plotted representing standard Gibbs free energy change for chromium oxides, as well as for FeO and MnO formation as a function of temperature (see Fig. **2**). It should be considered that Ellingham diagram is applied for the activity 1 and thus, gives relative estimation of the oxide's stabilities in the case of real slags. The corresponding activity ratios for the real slag systems are shown for FeO/Fe as 0.1 and 0.01 by the dashed lines (Fig. **3** left).

Gibbs free energy corresponding to the formation of Cr_2O oxide according to the reaction (2) has positive values. Cr_2O oxide has low melting point and can only be stable at low oxygen pressures under vacuum.

The Gibbs free energies of oxide's formation with a positive slope indicate that with the raising temperature the stability of oxides drops.

The lines corresponding to the formation of CrO_2 and CrO_3 oxides intersect. The cross area is presented on the Fig. **3** (right).

Cr_2O_3 is the most stable oxide according to the derived results, whilst Cr_2O and CrO are the least stable.

As reported by Wang and Seetharaman et al. [10] chromium oxide contamination from chromium-containing slags can take place in oxidizing atmosphere. The formation of Cr^{6+} can occur through a number of transformations from Cr^{2+} to Cr^{3+} first with further transformation to Cr^{6+}. Cr^{4+} formation was not indicated by experimental studies. The main chromium component in steel slag corresponds to the 2+ valency.

In this paper thermodynamic calculations for ladle furnace (LF), EAF and BOF slags has been carried out with FactSage 7.1. The composition of slags is presented in **Table 1**.

The first step of thermodynamic calculations for slags started with the simplified system CaO-SiO_2-Cr_2O_3-O_2 (see Fig. **4**), where Cr^{3+} containing phases were found like $CaCr_2O_4$, garnet and Ca spinel (highlighted in red)

As a next step, iron oxide was introduced as it is considerable constituent of many steel slags, especially BOF and EAF slag. Figure **5** presents the stability diagram for the BOF slag system CaO-SiO_2-Cr_2O_3-FeO-O_2 indicating various phases with respect to the composition, slag basicity CaO/SiO_2 in the range of 1.8 to 4 and temperature at constant oxygen partial pressure. Thermodynamic calculations for slag were carried out in the range of temperatures 700 - 2500 K and oxygen partial pressure for air. The Cr_2O_3 content fixed at 0.45%. Fact 53 and FToxid databases were used for the calculations.

In this system various phases are formed like olivine, dicalcium silicate, rankinite, brownmillerite, as well as Ca and Cr-based compounds such as $CaCr_2O_4$. According to FactSage calculations, the dominating phase is Cr^{3+} containing spinel. The domain of Cr^{3+} containing spinel phases has been highlighted in red (Fig.5). The early formation of chromium - Ca spinel phase has been presented in all cases and remains in the range of slag basicities from 1.8 to 4.

Figure **6** illustrates the diagram of oxygen partial pressure as a function of compositon for the system: CaO-SiO_2-Cr_2O_3-O_2-FeO. Isoactivity lines of CrO_3 oxide are plotted with a very low value indicating the instability of the compound and strong dependence on the oxygen partial pressure. Below the basicity 1 there were no chromium containing compounds found.

Based on recent study [3] Ca-Cr compounds are suggested to be easily leachable and thus there ia potential risk of emisison of Cr^{6+} from chromium containing phases. Authors pointed out that the addition of magnesia favors the formation of $MgCr_2O_4$ or $FeCr_2O_4$ phase where Cr is stabilized and slag becomes less vulnerable towards leaching.

Real slag systems in steelmaking usually comprise Al_2O_3, MgO and MnO as well. Figures **7** and **8** present the real multicomponent BOF slag in the system CaO-SiO_2-Cr_2O_3-O_2-FeO-Al_2O_3-MgO-MnO, where various phases were found like: Olivine, Ca_2SiO_4, monoxides, corundum, brownmillerite, $Ca_3(Al,Fe)_2O_6$, merwinite, melilite, spinel, andradide, $Ca_3MgAl_4O_{10}$ and Mn_2O_3.

Cr^{3+} valent Ca spinel phases were found belonging to the basicity range 1.8 - 2.1. With the presence of MgO, Al_2O_3 and MnO the domain of Cr^{3+} containing Ca spinel phase has been shortened and no hexavalent chromium containing compounds were indicated, whether oxygen partial pressure was for air or FeO-Fe equilibrium in slag. At higher basicity of 3 there was no Ca spinel phase. The results derived are consistent with conclusions made in the literature that in the range CaO/SiO_2 from 1.8 to 4 basicity is the influencing factor for the formation of spinel phase [2].

Figures **9** and **10** illustrate the stability diagrams for the EAF real multicomponent slag system $CaO\text{-}SiO_2\text{-}Cr_2O_3\text{-}O_2\text{-}FeO\text{-}Al_2O_3\text{-}MgO\text{-}MnO$. Same is shown for ladle furnace (LF) slag in Figures **11** and **12** respectively. Diagrams are calculated at constant oxygen partial pressure for FeO-Fe equilibrium conditions and air in the range of the slag basicities from 1.8 to 4. For the EAF slag the Cr_2O_3 content was fixed at 1.58 % and at 0.09 % for the ladle furnace slag. Phases like wollastonite, pseudo-wollastonite, dicalcium silicate, rankinite, brownmillerite, merwinite, melilite, spinel, andradide, $Ca_3MgAl_4O_{10}$ and Mn_2O_3 were found.

Cr^{3+} containing phase $CaCr_2O_4$ (Ca spinel) present in the EAF slag and is formed in the very small domain in the range of basicities from 1.8 to 2.4 (phase is marked in red in Fig. **9** and **10**). Therefore, the early formation of Cr containing Ca spinel phase is influenced by the basicity. In the case of LF slag, Ca spinel phase was not formed. Based on Factsage results, with the input data used, Cr^{6+} valent phases were not found at any oxygen partial pressure given.

Conclusions

According to the experimental studies and literature [2…4; 7; 8, 10] there is a potential risk for the Cr^{6+} formation in slags (especially stainless steel slags) under oxidizing conditions.

In this paper the thermodynamic estimation of various Cr oxides stabilities has been carried out. The $Cr\text{-}O_2$ stability diagram has been derived using FactSage 7.1. The CrO_3 oxide has not been indicated in the system.

The Ellingham diagram for chromium oxides has been plotted presenting the standard Gibbs free energy for corresponding oxides formation as a function of temperature. The stability of Cr_2O, CrO, Cr_2O_3 CrO_2 and CrO_3 oxides with the increase in temperature has been defined.

Stability diagrams of temperature versus composition at constant oxygen partial pressure for air and FeO-Fe equilibrium conditions in slag were plotted. Thermodynamic calculations were carried out with Factsage 7.1 for simplified and real multicomponent BOF, LF and EAF slags. The stability diagrams plotted for simplified slags ($CaO\text{-}SiO_2\text{-}Cr_2O_3\text{-}O_2$ and $CaO\text{-}SiO_2\text{-}Cr_2O_3\text{-}O_2\text{-}FeO$) showed multiple phases including dominant Cr^{3+} containing compounds without exavalent chromium.

Moreover, the presence of hexavalent Cr was also not found in real multicomponent systems (with the addition of MgO, Al_2O_3 and MnO) conforming to FactSage with the input data used, independent from oxygen partial pressure, i.e. for air or FeO-Fe equilibrium. Cr_2O_3 content was fixed at 0.09, 0.45 and 1.58 wt % corresponding to different slag compositions (BOF, LF and EAF). Cr^{3+} phase had small domain compared to theoretic slag systems in the range of slag basicity of 1.8 - 2.1.

It is worth mentioning, that the presence of FeO, Al_2O_3 and MgO in the slag system favors the stabilizaton of chromium phase with the oxygen partial pressure set for air and FeO-Fe equilibrium.

References

[1] H. Cheng, J. Wang, Y. Wan, H. Chen, an overview of utilization of steel slag, Procedia Environmental Sciences, The Seventh International Conference on Waste Management and Technology (ICWMT 7), Volume 16, 2012, pp. 791-801.

[2] G.J. Albertsson, Abatement of Chromium emissions from steelmaking slags - Cr stabilization by phase separation, Doctoral thesis. Royal Institute of Technology, Sweden 2013.

[3] Cabrera-Real, Hugo; Romero-Serrano, Antonio; Zeifert, Beatriz; Hernandez-Ramirez, Aurelio; Hallen-Lopez, Manuel; Cruz-Ramirez, Alejandro Effect of MgO and CaO/SiO on the immobilization of chromium in synthetic slags. Journal of Material Cycles & Waste Management . Oct2012, Vol. 14 Issue 4, p317-324. 8p.

[4] M. Kühn, D. Mudersbach: Scanmet II — 2nd Int. Conf. On Process Development in Iron and Steelmaking, Luleå, Sweden, 6.-9. June 2004, 369.

[5] D. Mudersbach, M. Kühn, J. Geisler, and K. Koch, ''Chrome immobilisation in EAF-slags from highalloy steelmaking: tests at FEhS institute and development of an operational slag treatment process'', Proceedings of 1st International Slag Valorisation Symposium, Leuven, Belgium 2009.

[6] S. Schüler, H. Markus, D. Algermissen, D. Mudersbach Electric arc furnace slag engineering during production, treatment, solidification and processing, Proceedings of 4th International Slag Valorisation Symposium in Leuven; 2015, p. 69-75.

[7] N. Sano, Reduction of Chromium Oxide in Stainless Steel Slags. Proceedings: Tenth International Ferroalloys Congress, 2004.

[8] K. Morita, A. Inoue, N. Takayama and N. Sano: Tetsu-to Hagane, 1988, vol. 74, pp. 59-65.

[9] Factsage 7.1 - Thermfact Ltd (Montreal, Canada) and GTT technologies Aachen, Germany, Database: fact53, FToxid.

[10] L.J. Wang and S. Seethraman: Metall. Mater. Trans. B, 2010, vol. 41B, pp. 946—54.

Figures

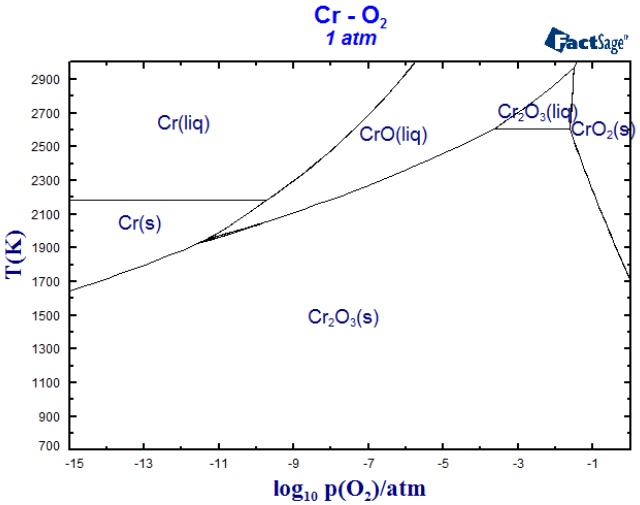

Figure 1: Cr-O_2 phase stability diagram plotted using Factsage 7.1

Cr-O_2 Phasendiagramm, dargestellt mittels Factsage 7.1

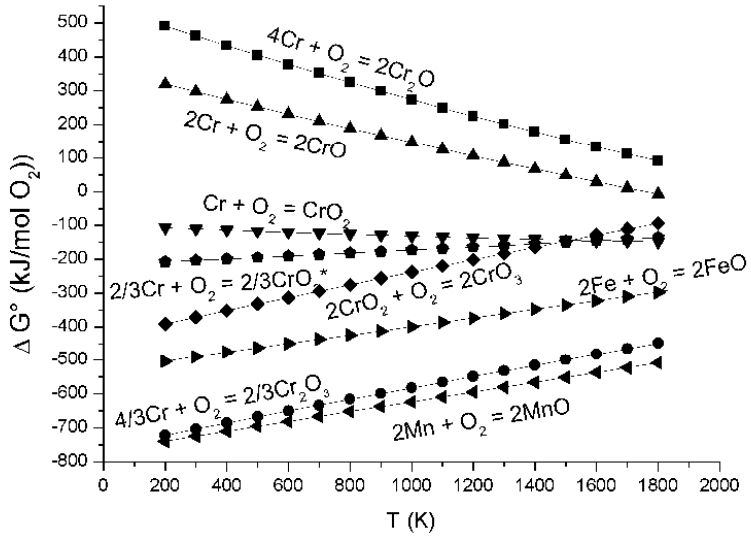

Figure 2: Ellingham diagram plotted using Factsage 7.1 for chromium oxides

Ellingham-Diagramm für Chromoxide, dargestellt mittels Factsage 7.1

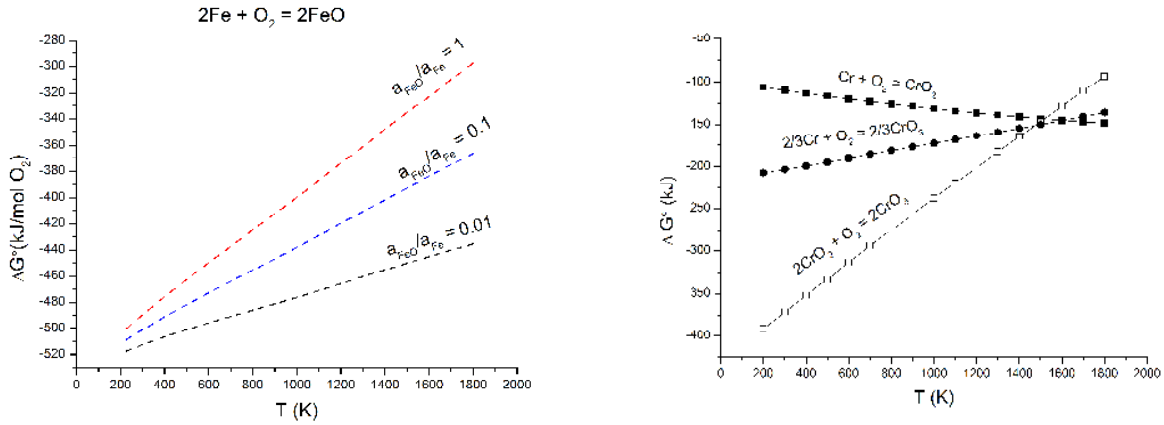

Figure **3**: FeO/Fe activity ratios (left), the cross area of the reactions (right)

FeO/Fe-Aktivitätsverhältnisse (links) und Schnittpunkt der Reaktionen (rechts)

Ladle slag	**Aver. wt %**	**BOF slag**	**Aver. wt %**	**EAF slag**	**Aver. wt %**
Fe	0.56	Fe	1.93	Fe	0.80
FeO	4.16	FeO	9.32	FeO	20.93
Fe_2O_3	0.68	Fe_2O_3	15.86	Fe_2O_3	9.75
CaO	33.60	CaO	46.47	CaO	29.58
SiO_2	15.16	SiO_2	14.12	SiO_2	14.49
MgO	12.95	MgO	2.92	MgO	6.99
Al_2O_3	14.35	Al_2O_3	2.37	Al_2O_3	5.67
Cr_2O_3	0.09	Cr_2O_3	0.45	Cr_2O_3	1.58
Cr(VI)	0.0001	Cr(VI)	0.0001	Cr(VI)	0.0001
MnO	6.67	MnO	3.53	MnO	5.26
P_2O_5	0.03	P_2O_5	1.02	P_2O_5	1.39
TiO_2	0.51	TiO_2	0.77	TiO_2	0.47

Table 1: The composition of ladle furnace, EAF and BOF slags

Chemische Zusammensetzungen der den Berechnungen zugrunde gelegten sekundärmetallurgischen Schlacke, Elektroofen- und LD-Schlacke

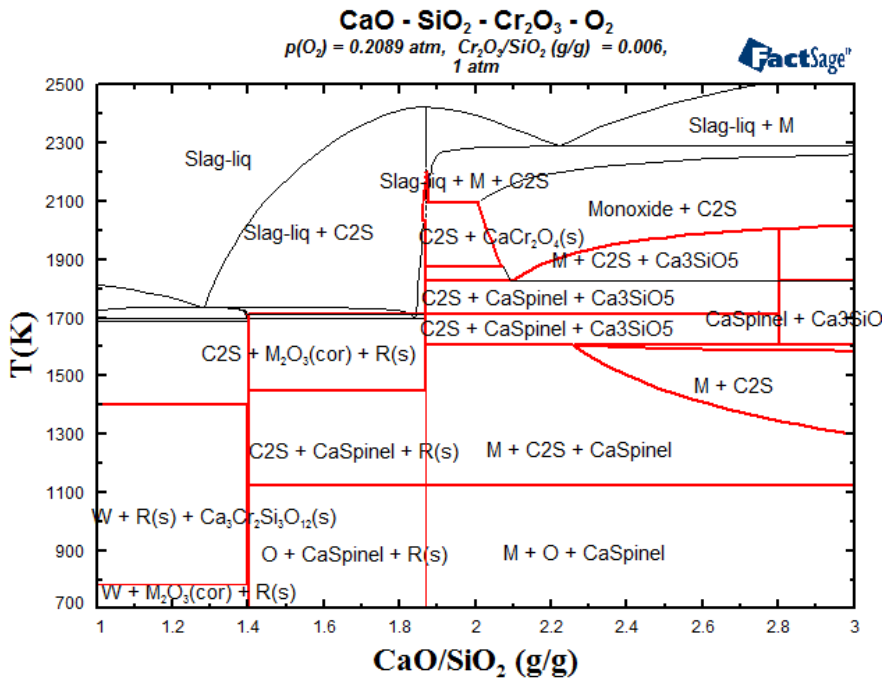

Figure 4: The stability diagram for the simplified slag system CaO-SiO_2-Cr_2O_3-O_2 and p_{O2} for air using Factsage 7.1

Phasendiagramm für das vereinfachte Schlackensystem CaO-SiO_2-Cr_2O_3-O_2 und pO2 für Luft gemäß Factsage 7.1

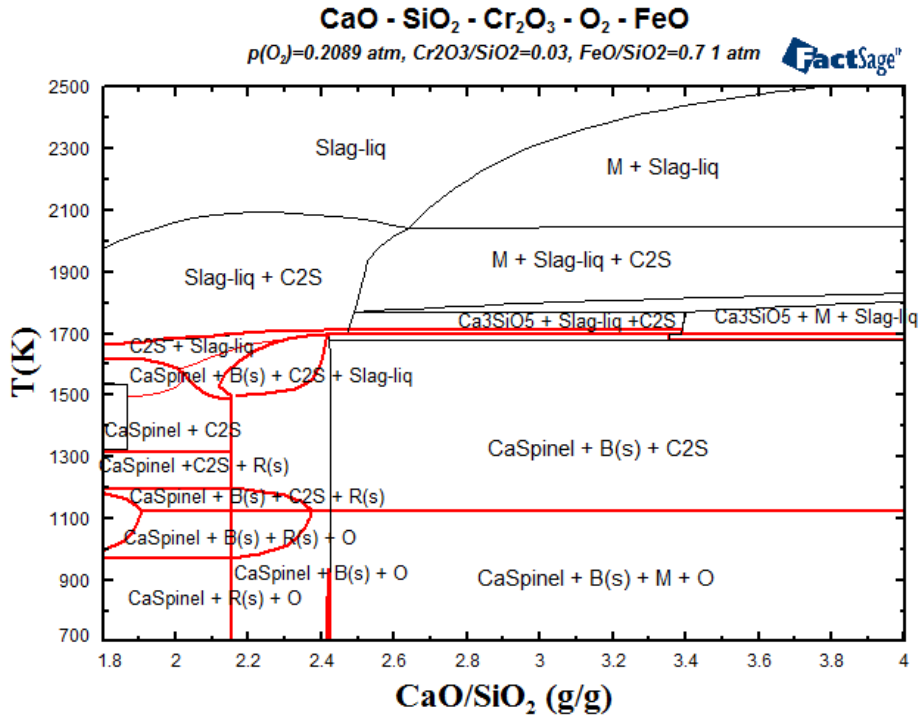

Figure 5: The stability diagram for the simplified slag system CaO-SiO_2-Cr_2O_3-O_2-FeO and p_{O2} for air using Factsage 7.1 (O - olivine, C_2S- α-Ca_2SiO_4, M- monoxide, B- brownmillerite, R- rankinite)

Phasendiagramm für das vereinfachte Schlackensystem CaO-SiO_2-Cr_2O_3-O_2-FeO und pO2 für Luft gemäß Factsage 7.1 (O — Olivin, C_2S — α-Ca_2SiO_4, M — Monoxid, B — Brownmillerit, R — Rankinit)

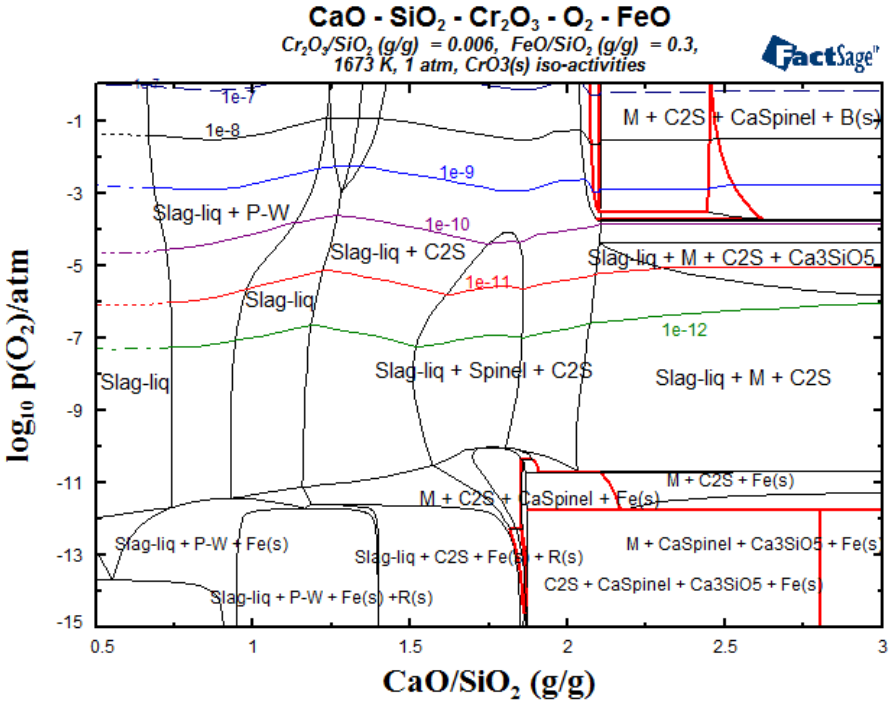

Figure 6: The stability diagram for the simplified system CaO-SiO_2-Cr_2O_3-O_2-FeO using Factsage 7.1 (C_2S- α-Ca_2SiO_4, M- monoxide, P-W - pseudo-wollastonite)

Phasendiagramm für das vereinfachte Schlackensystem CaO-SiO_2-Cr_2O_3-O_2-FeO gemäß Factsage 71. (C_2S — α-Ca_2SiO_4, M — Monoxid, P-W - Pseudowollastonit)

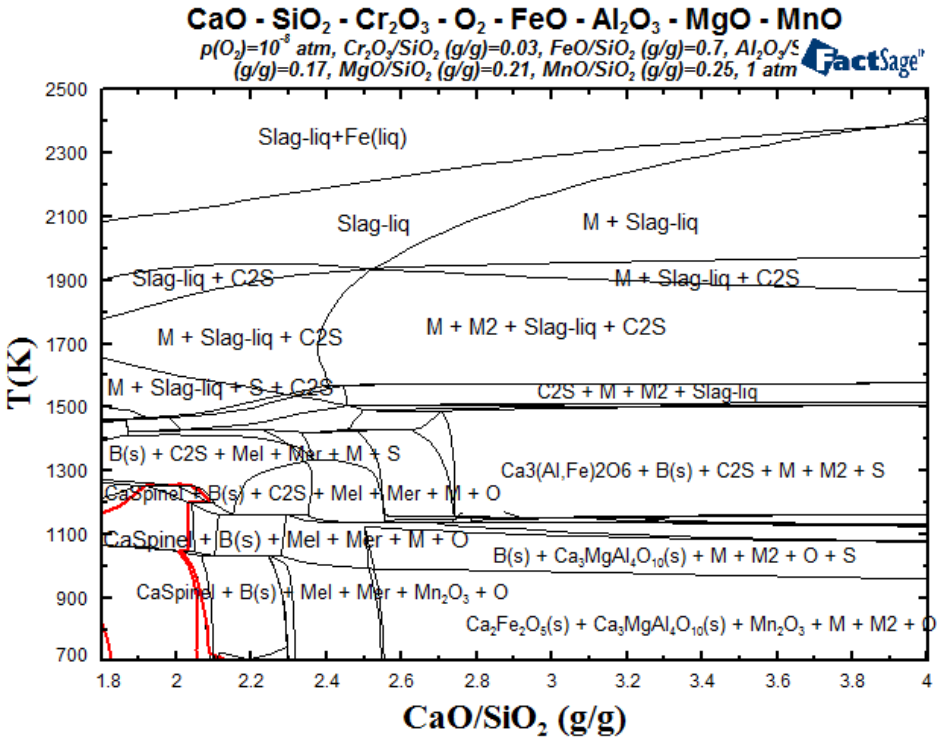

Figure 7: The stability diagram for the BOF slag system CaO-SiO_2-Cr_2O_3-O_2-FeO-Al_2O_3-MgO-MnO and p_{O2} for FeO-Fe equilibrium using Factsage 7.1 (O - olivine, C_2S- α-Ca2SiO4, M and M2-monoxides, B- brownmillerite, Mer- merwinite, Mel — melilite, S- spinel)

Phasendiagramm für das LD-Schlackensystem $CaO\text{-}SiO_2\text{-}Cr_2O_3\text{-}O_2\text{-}FeO\text{-}Al_2O_3\text{-}MgO\text{-}MnO$ und pO2 für das Gleichgewicht FeO-Fe gemäß Factsage 7.1 (O — Olivin, C_2S — $\alpha\text{-}Ca_2SiO_4$, M and M2 — Monoxid, B — Brownmillerit, Mer —Merwinit, Mel — Melilith, S - Spinell)

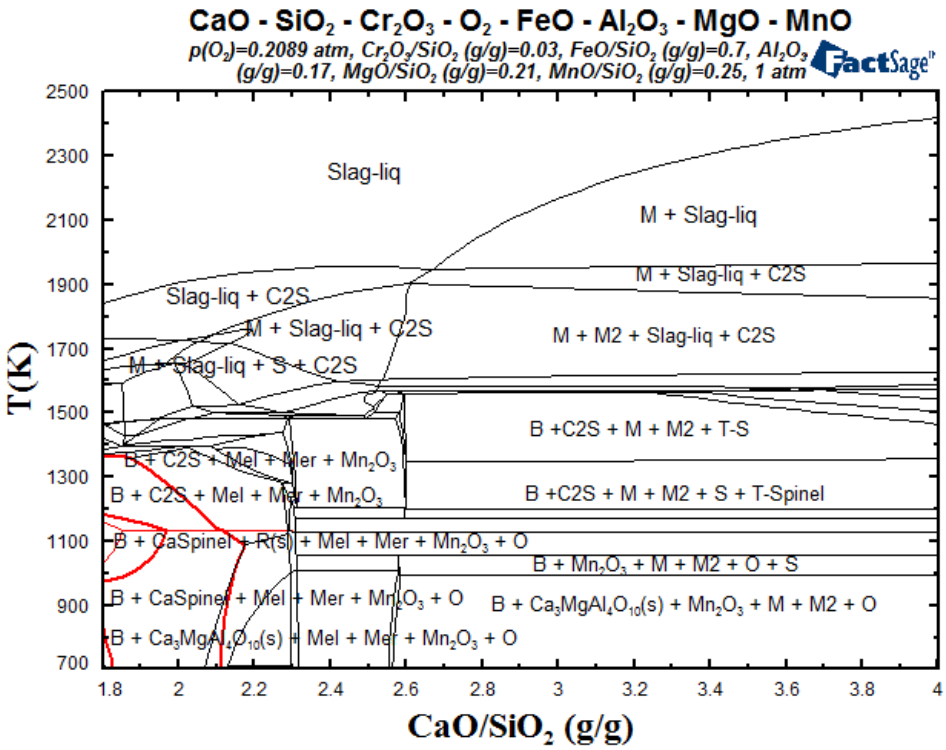

Figure 8: The stability diagram for the BOF slag system $CaO\text{-}SiO_2\text{-}Cr_2O_3\text{-}O_2\text{-}FeO\text{-}Al_2O_3\text{-}MgO\text{-}MnO$ and p_{O2} for air using Factsage 7.1 (O-olivine, C_2S- α-Ca2SiO4, M and M2- monoxides, B-brownmillerite, Mer- merwinite, Mel — melilite, S- spinel, T-Spinel- tetragonal spinel — the phase name is considered an error in the database)

Phasendiagramm für das LD-Schlackensystem $CaO\text{-}SiO_2\text{-}Cr_2O_3\text{-}O_2\text{-}FeO\text{-}Al_2O_3\text{-}MgO\text{-}MnO$ und pO2 für Luft gemäß Factsage 7.1 (O — Olivin, C_2S — $\alpha\text{-}Ca_2SiO_4$, M and M2 — Monoxid, B — Brownmillerit, Mer —Merwinit, Mel — Melilith, S - Spinell)

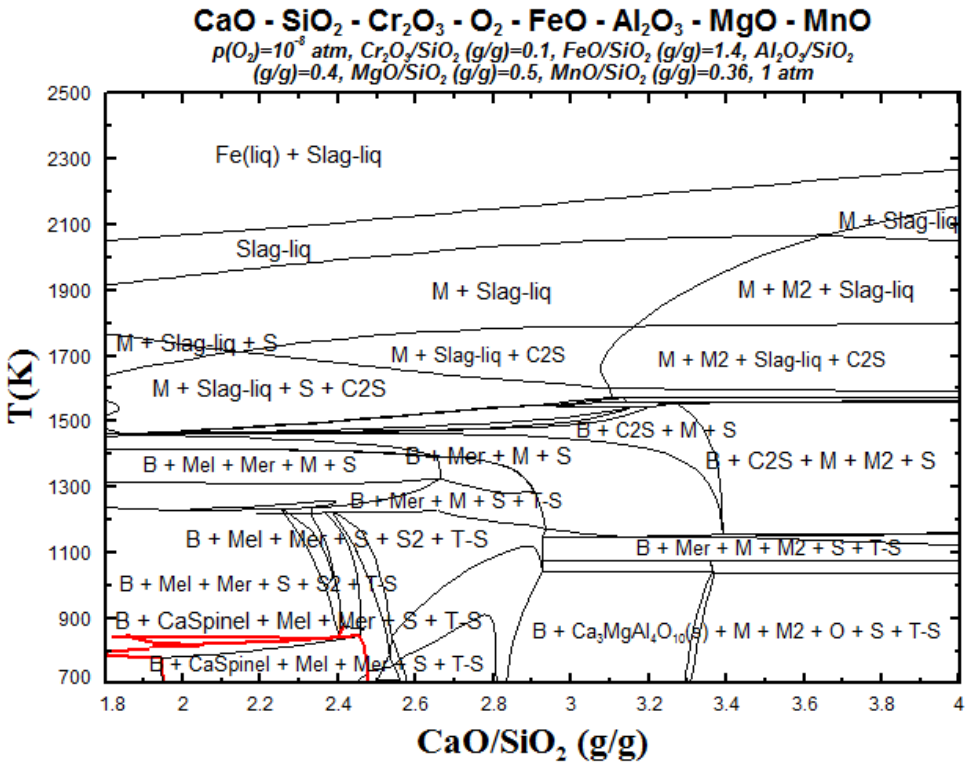

Figure 9: The stability diagram for the EAF slag system CaO-SiO_2-Cr_2O_3-O_2-FeO Al_2O_3-MgO-MnO and p_{O2} for FeO-Fe equilibrium in slag using Factsage 7.1 (O - olivine, C_2S- α- Ca_2SiO_4, M, M2 - monoxides, B- brownmillerite, Mel — melilite, Mer- Merwinite, S — spinel)

Phasendiagramm für das Elektroofen-Schlackensystem CaO-SiO_2-Cr_2O_3-O_2-FeO-Al_2O_3-MgO-MnO und pO2 für das Gleichgewicht FeO-Fe gemäß Factsage 7.1 (O — Olivin, C_2S — α-Ca_2SiO_4, M, M2 — Monoxide, B — Brownmillerit, Mer —Merwinit, Mel — Melilith, S - Spinell)

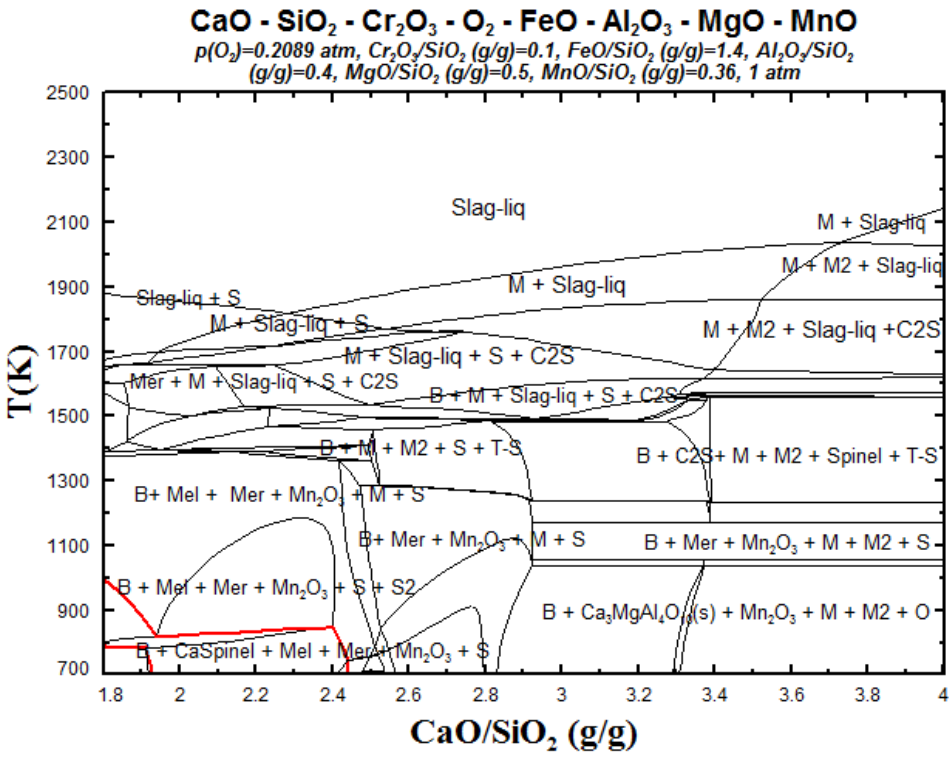

Figure 10: The stability diagram for the EAF slag system $CaO\text{-}SiO_2\text{-}Cr_2O_3\text{-}O_2\text{-}FeO\ Al_2O_3\text{-}MgO\text{-}MnO$ and p_{O2} for air using Factsage 7.1 (O - olivine, C_2S- α- Ca_2SiO_4, M, M2 - monoxides, B- brownmillerite, Mel — melilite, Mer- Merwinite, S — spinel)

Phasendiagramm für das Elektroofen-Schlackensystem $CaO\text{-}SiO_2\text{-}Cr_2O_3\text{-}O_2\text{-}FeO\text{-}Al_2O_3\text{-}MgO\text{-}MnO$ und p_{O2} für Luft gemäß Factsage 7.1 (O — Olivin, C_2S — α-Ca_2SiO_4, M, M2 — Monoxide, B — Brownmillerit, Mer —Merwinit, Mel — Melilith, S - Spinell)

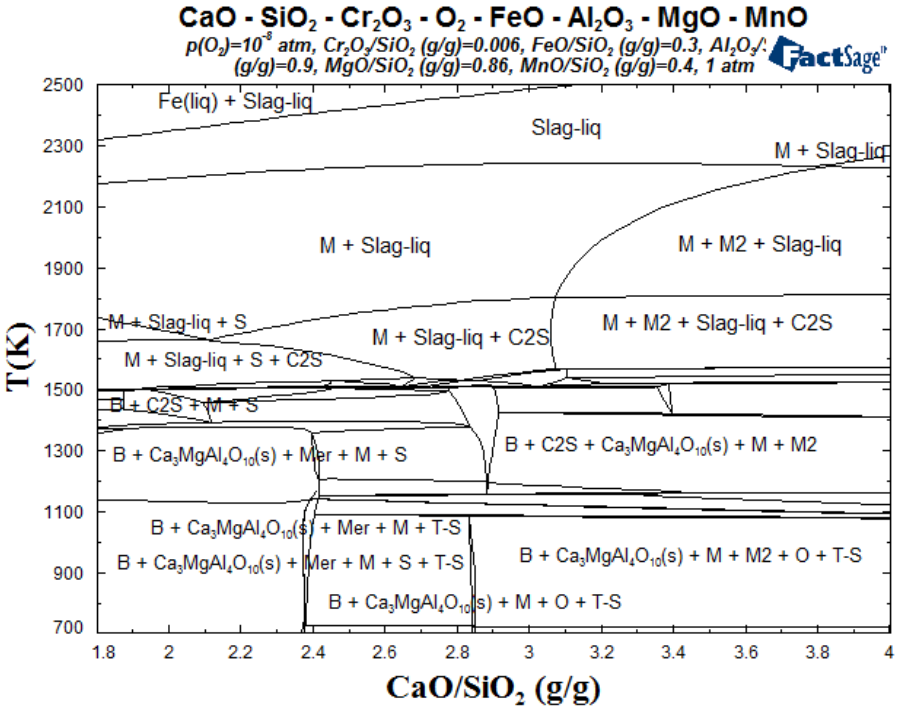

Figure 11: The stability diagram for the ladle furnace slag system $CaO\text{-}SiO_2\text{-}Cr_2O_3\text{-}O_2\text{-}FeO\ Al_2O_3\text{-}MgO\text{-}MnO$ and p_{O2} for FeO-Fe equilibrium using Factsage 7.1 (O - olivine, C_2S- α- Ca_2SiO_4, M, M2- monoxides, B- brownmillerite, Mer — merwinite, S —spinel)

Phasendiagramm für das sekundärmetallurgische Schlackensystem $CaO\text{-}SiO_2\text{-}Cr_2O_3\text{-}O_2\text{-}FeO\text{-}Al_2O_3\text{-}MgO\text{-}MnO$ und p_{O2} für das Gleichgewicht FeO-Fe gemäß Factsage 7.1 (O — Olivin, C_2S — α-Ca_2SiO_4, M, M2 — Monoxide, B — Brownmillerit, Mer —Merwinit, Mel — Melilith, S - Spinell)

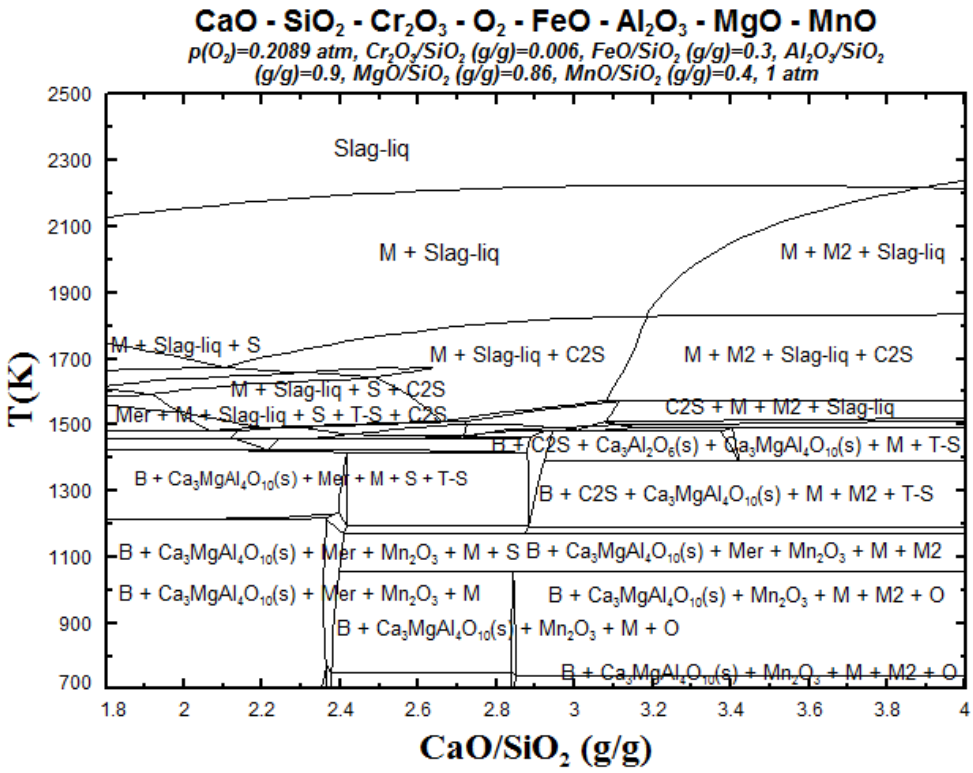

Figure **12**: The stability diagram for the ladle furnace slag system CaO-SiO_2-Cr_2O_3-O_2-FeO Al_2O_3-MgO-MnO and p_{O2} for air using Factsage 7.1 (O - olivine, C_2S- α- Ca_2SiO_4, M, M2- monoxides, B- brownmillerite, Mer - merwinite, S — spinel)

Phasendiagramm für das sekundärmetallurgische Schlackensystem CaO-SiO_2-Cr_2O_3-O_2-FeO-Al_2O_3-MgO-MnO und p_{O2} für Luft gemäß Factsage 7.1 (O — Olivin, C_2S — α-Ca_2SiO_4, M, M2 — Monoxide, B — Brownmillerit, Mer —Merwinit, Mel — Melilith, S - Spinell)